Talanta 156-157 (2016) 172–179

Contents lists available at ScienceDirect

Talanta

journal homepage: www.elsevier.com/locate/talanta

An electrochemical genosensor for *Leishmania major* detection based on dual effect of immobilization and electrocatalysis of cobalt-zinc ferrite quantum dots

H. Heli [a,*], N. Sattarahmady [a,b], G.R. Hatam [c,d], F. Reisi [a,e], R. Dehdari Vais [a]

[a] Nanomedicine and Nanobiology Research Center, Shiraz University of Medical Sciences, Shiraz, Iran
[b] Department of Medical Physics, School of Medicine, Shiraz University of Medical Sciences, Shiraz, Iran
[c] Department of Parasitology and Mycology, School of Medicine, Shiraz University of Medical Sciences, Shiraz, Iran
[d] Basic Sciences in Infectious Diseases Research Center, Shiraz University of Medical Sciences, Shiraz, Iran
[e] Department of Nanomedicine, School of Advanced Medical Sciences and Technologies, Shiraz University of Medical Sciences, Shiraz, Iran

ARTICLE INFO

Article history:
Received 9 March 2016
Received in revised form
27 April 2016
Accepted 28 April 2016
Available online 7 May 2016

Keywords:
Signal-on genosensor
DNA biosensor
Ferrite
Electrocatalysis
Magnetic nanoparticles

ABSTRACT

Identification of *Leishmania* parasites is important in diagnosis and clinical studies of leishmaniasis. Although epidemiological and clinical methods are available, they are not sufficient for identification of causative agents of leishmaniasis. In the present study, quantum dots of magnetic cobalt-zinc ferrite ($Co_{0.5}Zn_{0.5}Fe_2O_4$) were synthesized and characterized by physicochemical methods. The quantum dots were then employed as an electrode modifier to immobilize a 24-mer specific single stranded DNA probe, and fabrication of a label-free, PCR-free and signal-on electrochemical genosensor for the detection of *Leishmania major*. Hybridization of the complementary single stranded DNA sequence with the probe under the selected conditions was explored using methylene blue as a redox marker, utilizing the electrocatalytic effect of the quantum dots on the methylene blue electroreduction process. The genosensor could detect a synthetic single stranded DNA target in a range of 1.0×10^{-11} to 1.0×10^{-18} mol L^{-1} with a limit of detection of 2.0×10^{-19} mol L^{-1}, and genomic DNA in a range of 7.31×10^{-14} to 7.31×10^{-6} ng μL^{-1} with a limit of detection of 1.80×10^{-14} ng μL^{-1} with a high selectivity and sensitivity.

1. Introduction

Rapid, sensitive and simple determination methods of special gene sequence in very small sample volumes have attracted increasing attention in the diagnosis of genetic and infectious diseases, and detection of pathogenic microorganisms. Conventional DNA detection methods, i.e. PCR, gel electrophoresis and Southern blotting are labor intensive and time consuming [1–3]. Therefore, many techniques such as surface-enhanced Raman scattering [4], surface Plasmon resonance spectroscopy [5], fluorescence spectroscopy [6], UV–vis spectroscopy [7] and electrochemistry [8–11] have been developed for DNA detection. Among them, the electrochemical methods have recently received a good deal of attention due to the inherent specificity and sensitivity, their ease of use, low cost, fast response, and miniaturized and automated devices [8,9,12].

For many years, the appropriate modification of the conductive surfaces to immobilize biomacromolecules (such as DNA) has been one of the important approaches in biotechnology, bioanalysis, nanomedicine, and fabrication of biosensors [13–18]; it is also useful in understanding the action mechanism of drugs and origin of some diseases [19–21]. In a DNA biosensor, the immobilization of a DNA probe on the surface of an electrode is a key step and up to now, various kinds of nanostructured materials have been devised for the single-stranded DNA (ssDNA) immobilization [8,9,22,23]. This is due to their physicochemical properties to be highly tunable depending on their size and shape, unique surface chemistry, thermal stability, high surface area as well as good biocompatibility enabled by their nanometer sizes [12,24–28]. In this regard, magnetic nanostructures due to modulation in the chemical composition, size and magnetic susceptibility and good dispersibility are important for use in a variety of biosensing systems [29,30].

Cutaneous leishmaniasis is a group of protozoan infections caused by obligate intracellular protozoan parasites. These skin diseases occur in particular endemic regions in at least 88 countries of the world [31,32]. Annual incident of cutaneous leishmaniasis is estimated to be 1–1.5 million cases.

* Corresponding author.
E-mail addresses: hheli7@yahoo.com, heli@sums.ac.ir (H. Heli).

http://dx.doi.org/10.1016/j.talanta.2016.04.065
0039-9140/

Various laboratory methods are used to identify leishmaniasis, detect the parasite, and identify the *Leishmania* species [33–35]. Although epidemiological and clinical findings are necessary, they are not sufficient for identification of causative agents of cutaneous leishmaniasis. Diagnostic tests include light-microscopic examination of stained slides, in vitro culture from biopsy or lymph aspirate, Montenegro skin test, serological tests (including indirect fluorescent antibody test, enzyme-linked immunosorbent assay (ELISA) and isoenzyme analysis), and molecular tests (such as PCR). These methods are not sensitive enough or are indirect, require culture of the parasites or passage through an experimental animal which is time-consuming and sometimes unsuccessful. The antibody-based tests cannot detect early infections and distinguish between past and present infections, and cross-react with antibodies against other pathogens [36,37].

In the present study, quantum dots of magnetic cobalt-zinc ferrite ($Co_{0.5}Zn_{0.5}Fe_2O_4$) were synthesized and employed to modify a carbon paste electrode. A 24-mer specific sequence was immobilized to fabricate a label-free *Leishmania major* genosensor. The ability of the genosensor to detect *Leishmania major* in patient samples was investigated.

2. Experimental section

All chemicals were of analytical grade from Scharlau (Spain) or Sigma (USA) and were used without further purification. All solutions were prepared by redistilled water. A probe oligonucleotide (p-ssDNA) was designed based on the genomic sequence of *Leishmania major*. (p-ssDNA) was designed using NCBI BLAST nucleotide search tool and Primer3 based on a submitted sequence in GenBank (AB678349.1) of *Leishmania major* minicircle kDNA (Iranian Standard strain MCAN/IR/97/LON490, isolate: Iran JWmaj) [38]. The (p-ssDNA) sequence was evaluated for any possible homology and share sequences with any non-*Leishmania major* species using the BLAST of NCBI. In addition, the melting temperature of (p-ssDNA) was placed within a narrow range using Oligo analysis software. Finally, the (p-ssDNA) sequence was checked for the formation of potential self-dimer and secondary structures using mfold software (http://mfold. rna. albany. edu) [39] which may otherwise hinder the assay.

(p-ssDNA) was ordered from SinaClon BioScience Co. (Iran). A complementary-sequence oligonucleotide (target oligonucleotide, t-ssDNA) was purchased from SinaClon BioScience Co. (Iran). The oligonucleotide sequences were as follows:

(p-ssDNA) sequence: 5′-TGTTGGGTGACGCTTTAGTGGGTT-3′.

t-ssDNA sequence: 5′-AACCCACTAAAGCGTCACCCAACA-3′.

The oligonucleotide stock solutions were prepared with 20 mmol L^{-1} Tris–HCl buffer, pH 7.4 solution (Tris) and kept frozen.

Quantum dots of magnetic cobalt-zinc ferrite ($Co_{0.5}Zn_{0.5}Fe_2O_4$) were synthesized by a precipitation route. Co(II), Zn(II) and Fe(III) chloride salts with a 1:1:4 stoichiometric ratios were dissolved in a 100 mmol L^{-1} hydrochloric acid solution and heated to 80 °C. Then, a solution of 4.0 mol L^{-1} of sodium hydroxide with a temperature of 80 °C was rapidly added to the salts solution and

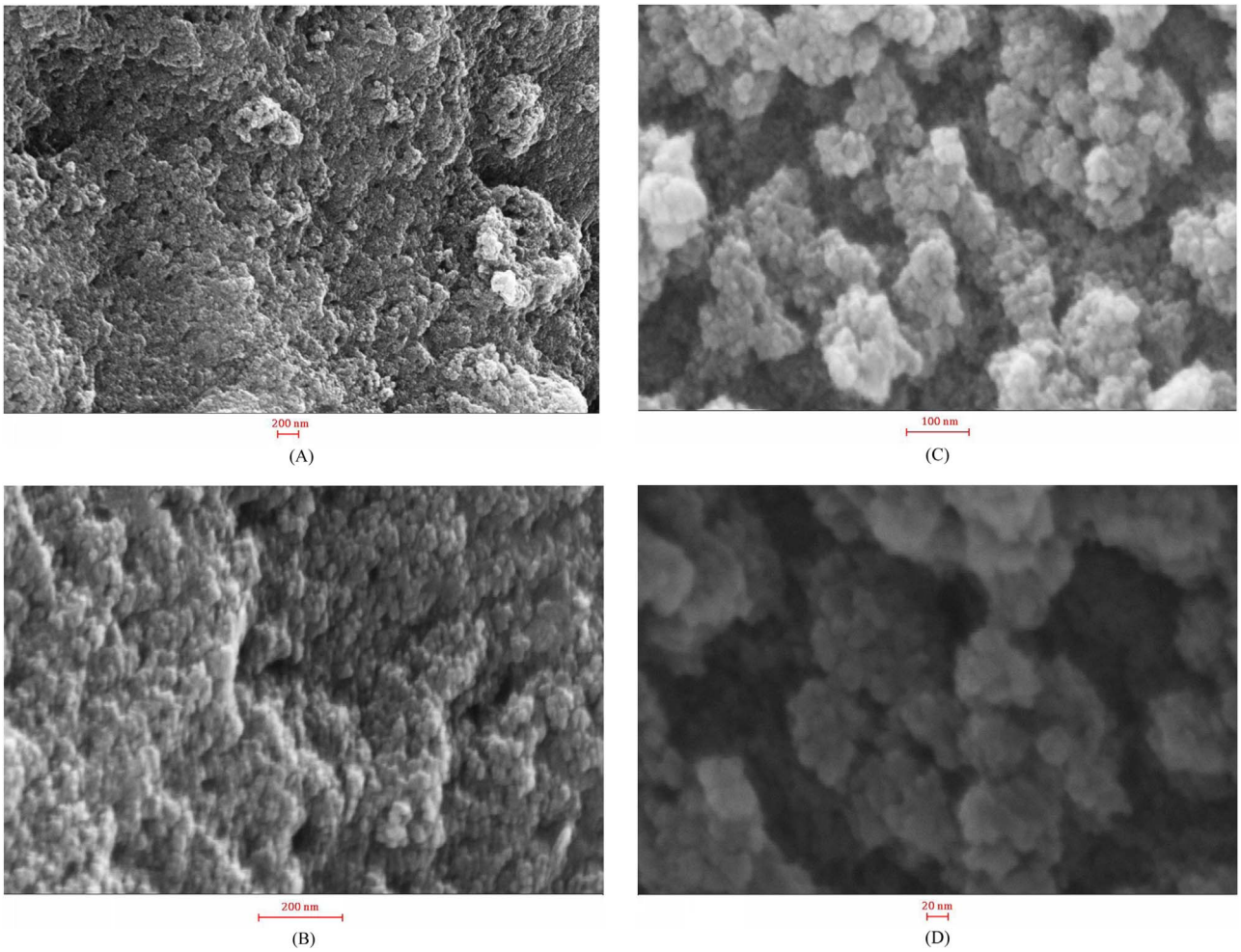

Fig. 1. FESEM images of magnetic cobalt-zinc ferrite quantum dots with different magnifications.

mixed with magnetic stirring to attain a final pH 12.0. The temperature was then increased to 100 °C and stirring was continued for 1 h to perform crystallization of the ferrite dots. The solution was then cooled to room temperature and the sample was collected by a permanent magnet. The sample was washed with water to neutralize the supernatant and dried at ambient temperature.

Field emission scanning electron microscopy (FESEM) was performed using a Zeiss, Sigma-IGMA/VP (Germany). A dried sample of the quantum dots was placed on a glass lamella, coated by a gold thin film, and observed under the microscope. Transmission electron microscopy (TEM) was carried out by a ZEISS instrument, EM 10C (Germany) with an accelerating voltage of 80 kV. A quantum dots suspension in water was ultrasonicated by a probe ultrasound for 45 min, and a droplet of the resultant suspension was placed on a TEM grid, and observed by TEM.

Electrochemical measurements were performed in a conventional three-electrode cell powered by a μ-Autolab potentiostat/galvanostat run by a computer through GPES 4.9 software. An Ag/AgCl, 3 mol L^{-1} KCl, and a platinum rod were used as the reference and counter electrodes, respectively.

Electrochemical detection of the DNA hybridization was performed in a 10 mL solution of Tris by cyclic voltammetry and differential pulse voltammetry for the reduction peak of bound

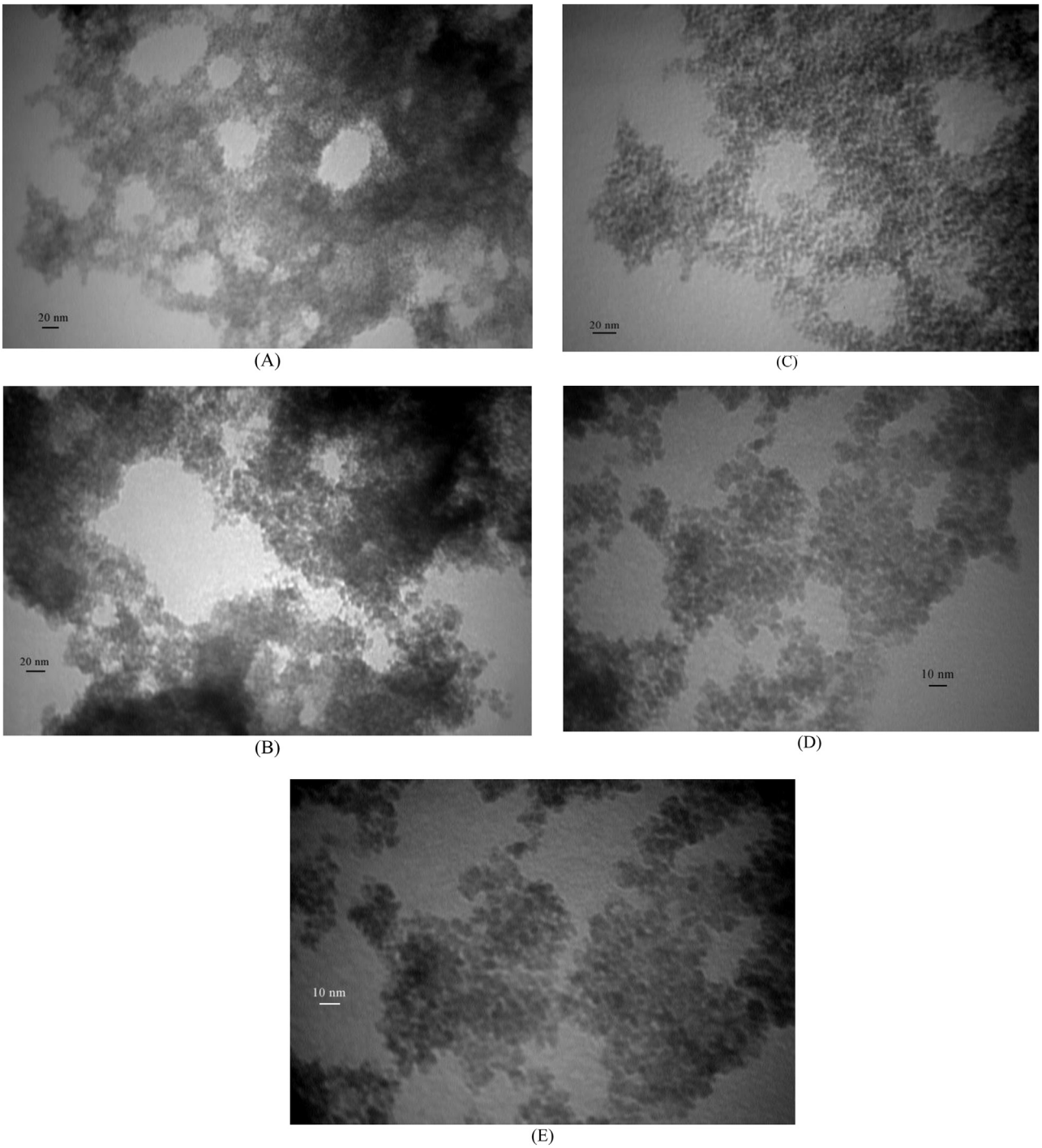

Fig. 2. TEM images of magnetic cobalt-zinc ferrite quantum dots with different magnifications.

methylene blue (MB). For differential pulse voltammetry, a pulse width of 25 mV, a pulse time of 50 ms, and a scan rate of 10 mV s^{-1} were employed. The concentrations of target DNA were quantified as the MB reduction peak current.

Unmodified carbon paste electrode (UCPE) was prepared by careful hand-mixing graphite fine powder and mineral oil with a ratio of 80:20 by wt%. The paste was packed firmly into a cavity (2 mm diameter) at the end of a Teflon tube. Electrical contact was established by a copper wire.

Modified carbon paste electrode (MCPE) with magnetic cobalt-zinc ferrite quantum dots were prepared by careful hand-mixing graphite fine powder, mineral oil, and cobalt-zinc ferrite quantum dots with ratios of 60:20:20 (wt%, otherwise stated) and the electrode was prepared similar to UCPE. When the percentage of the modifier was changed (optimization of the modifier amount), the summation of carbon powder and the modifier was kept to be at 80%. The surface of carbon paste electrodes was smoothed on a piece of weighing paper.

Immobilization of (p-ssDNA) was performed by dropping 10 µL of 7 µmol L^{-1} (p-ssDNA) solution dissolved in Tris on the MCPE surface, and remained intact under an IR lamp to dry [13]. The electrode was then rinsed thoroughly with Tris to remove the unadsorbed (p-ssDNA). The resultant electrode was denoted as the genosensor. Control experiments were also performed by UCPE.

The hybridization process was performed by dropping 10 µL of Tris containing various concentrations of t-ssDNA on the genosensor surface for 40 min at 37 °C. During this procedure, a small vial was tightly fit on the genosensor body to prevent quick evaporation of the droplet. Then, the electrode was rinsed with Tris to remove the unhybridized t-ssDNA, and then it was incubated in a solution containing Tris +20 µmol L^{-1} MB for 5 min at 37 °C [8]. Finally, the electrode was rinsed with Tris to remove the physically adsorbed MB.

The cryopreserved *Leishmania major* (MRHO/IR/75/ER) and *Leishmania infantum* (MCAN/IR/96/LON49) and *Leishmania tropica* (MHOM/IR/02/Mash10) were received from Tehran University of Medical Sciences, Tehran, Iran, and cultivated in RPMI 1640 medium supplemented with 10% (v/v) heat-inactivated fetal bovine serum (Gibco) and 1% pen-strep (Sigma) at 24 °C. The promastigotes were counted daily in a Neubauer chamber until a concentration of 1×10^7 mL^{-1} parasites was reached. Approximately, 10^7 phase promastigotes of isolates were harvested from the culture by centrifugation. The pellets were washed 3–4 times with chilled 50 mmol L^{-1} phosphate buffer saline (pH 7.0% and 0.7% NaCl) and suspended in 750 mL of NET buffer (5 mol L^{-1} NaCl, 0.5 mol L^{-1} EDTA, 1 mol L^{-1} Tris buffer pH 8.0). The cells were lysed with Proteinase K (100 mg mL^{-1}) and 1% sodium dodecyl sulphate for 3–4 h at 56 °C. Total DNA was extracted by the YTA Genomic DNA extraction mini kit (Yekta Tajhiz Azma, Iran) following the manufacturer's instructions, and DNA was eluted in 100–150 µL of elution buffer. The parasitic DNA concentration was determined by a Thermo Scientific NanoDrop 2000c (USA) and then diluted in a serial dilutions from 7.31×10^{-14} to 7.31×10^{-6} ng μL^{-1}.

Biopsy specimen of 6 human samples with cutaneous leishmaniasis was collected after sterilization of the lesion area on the slides, stained by Giemsa and microscopically characterized. Parasite DNA was extracted from 100 to 200 µL of the infected blood samples by the YTA Genomic DNA extraction Mini kit (Yekta Tajhiz Azma, Iran) following the manufacturer's instructions, and DNA was eluted in 100–150 µL of the elution buffer.

PCR followed by gel electrophoreses was performed to identify *Leishmania major* and *Leishmania tropica* in the human samples with cutaneous leishmaniasis. PCR primers were based on the non-protein coding region (AB678349.1) of *Leishmania major* minicircle kDNA (Iranian Standard strain MCAN/IR/97/LON490, isolate: IranJWmaj) gene region [38], and purchased from Sinaclon, Iran. The YTA kit for tissue was employed.

3. Results and discussion

Fig. 1 shows FESEM images of the magnetic cobalt-zinc ferrite quantum dots with different magnifications. In the dried sample of quantum dots, the particles were agglomerated due to their magnetic property. A mean diameter of 18 (± 3.3, n=200) nm was obtained for the individual agglomerated particles. Fig. 2 represents TEM images of the quantum dots with different magnifications. TEM images clearly show that the sample contains uniform particles with a narrow distribution size and a mean diameter of 4.2 (± 0.9, n=200) nm. Therefore, the ferrite sample is denoted as ferrite quantum dots.

Fig. 3 shows cyclic voltammograms recorded using UCPE and MCPE for 50 µmol L^{-1} MB in Tris. MB represents a couple peak of oxidation/reduction with a quasi-reversible kinetics on both the electrodes. However, the reduction peak current of MB on MCPE increased followed by decrement in the anodic peak current, compared to UCPE. This is a typical behavior for a surface redox mediation electron transfer process [40], indicating that the electroreduction of MB was catalyzed by one of the chemical species present in the quantum dots composition (EC' mechanism [40], Co (III) or Fe(III) species). This electrocatalytic process is supported by the dependency of the current function (peak current divided by the square root of the potential sweep rate) on the square root of the potential sweep rate, obtained by recording voltammograms of MB using MCPE at various potential sweep rates (Fig. 3, inset). Without going to the details of this process (which needs a detailed study), it causes a useful behavior in the fabrication of the genosensor by an enhancement in the reduction current of MB and increase in the sensitivity of the genosensor.

The cobalt-zinc ferrite quantum dots employed in this study provide a suitable surface to fabricate the genosensor. The quantum dots have an electrocatalytic effect toward the electroreduction of MB resulting in a higher peak current and sensitivity. On the other hand, they provide a high surface area due to the much small size to immobilize a high level of (p-ssDNA) and provide a high surface concentration of the probe. It has been reported that cobalt ferrite strongly and directly interacts with DNA and stabilizes its structure [41,42]; this leads to an application of ferrites to isolation and separation of DNA [16,43].

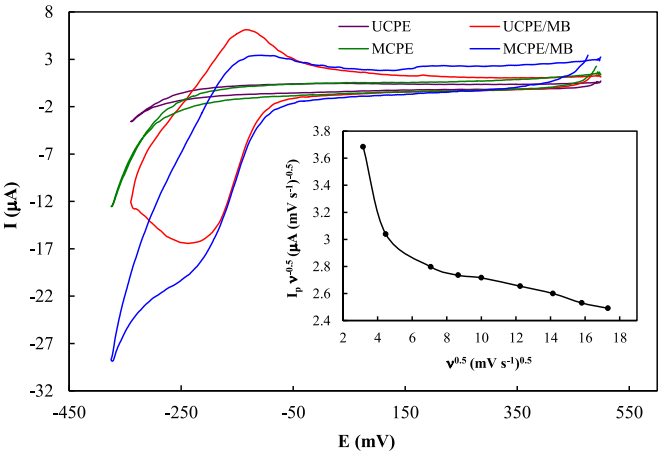

Fig. 3. Cyclic voltammograms recorded using UCPE and MCPE in the absence and presence of 50 µmol L^{-1} MB in Tris. The potential sweep rate was 50 mV s^{-1}. Inset: Dependency of current function on the square root of the potential sweep rate. The data was obtained from voltammograms of 50 µmol L^{-1} MB using MCPE recorded at various potential sweep rates.

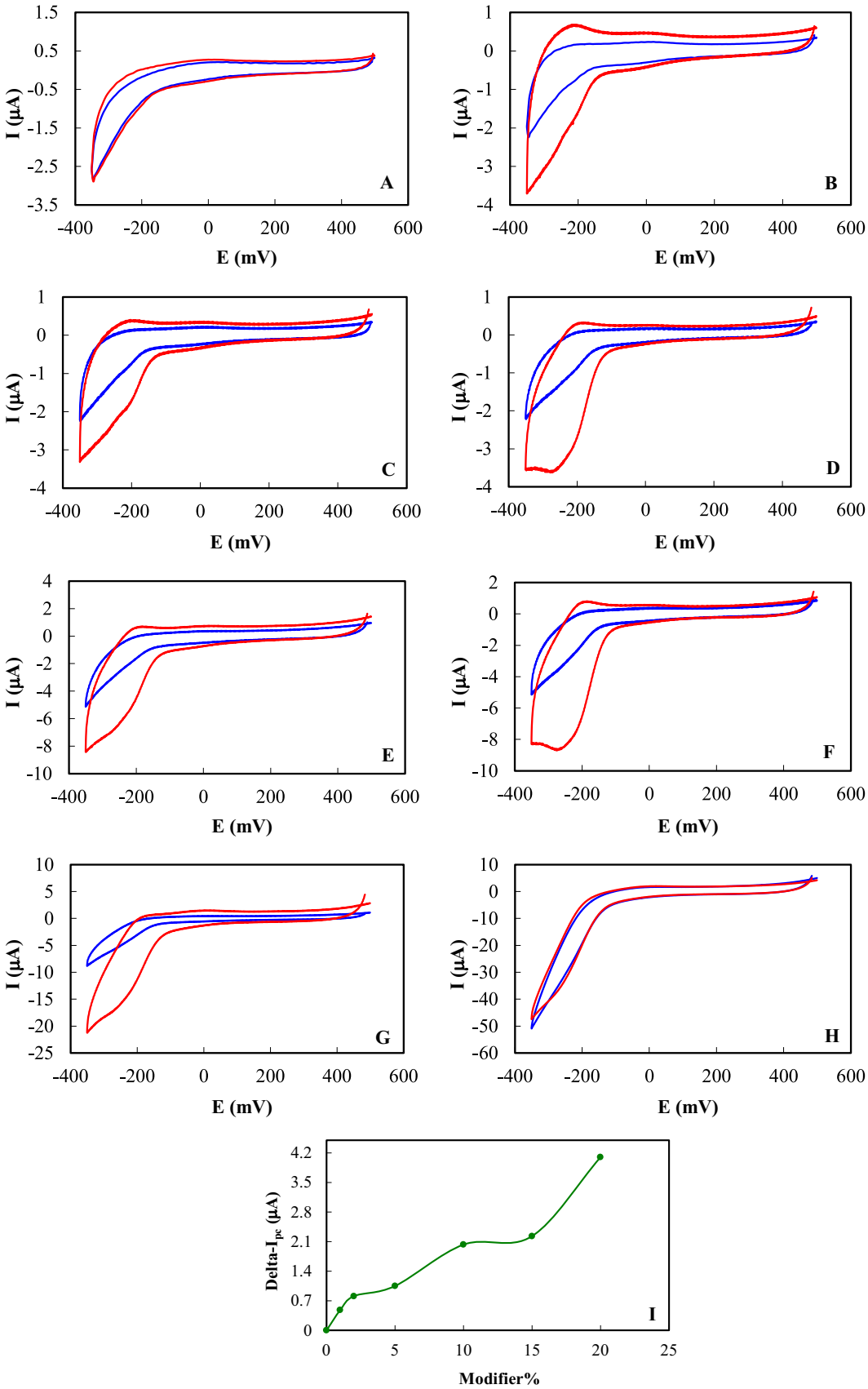

Fig. 4. A–H) Cyclic voltammograms of MB recorded using UCPE (A), and MCPEs prepared with different percent of the quantum dots of 1 (B), 2 (C), 5 (D), 10 (E), 15 (F), 20 (G), and 40% (H), after immobilization of (p-ssDNA) by dropping 10 μL of 7 μmol L^{-1} (p-ssDNA) solution dissolved in Tris on the electrode surfaces (blue curves) and subsequent by hybridization (red curves) with 10 μL of 1.0×10^{-13} μmol L^{-1} t-ssDNA solution dissolved in Tris for 40 min at 37 °C. The potential sweep rate was 50 mV s^{-1}. Probe-immobilized electrodes, before and also after hybridization process, were incubated in a solution containing Tris +20 mmol 20 μmol L^{-1} MB for 5 min at 37 °C, and then cyclic voltammograms were recorded. I) The dependency of the differences between the cathodic peak currents before and after hybridization on the modifier (quantum dots) percent. (For interpretation of the references to color in this figure legend, the reader is referred to the web version of this article.)

In order to optimize the experimental conditions to attain the best result (signal), the percentage of the quantum dots to prepare MCPE, concentration of (p-ssDNA) for the immobilization process, and the time of hybridization were optimized. Fig. 4(A–H) represents cyclic voltammograms of MB recorded using UCPE, and MCPEs prepared with different percentages of the quantum dots after immobilization of (p-ssDNA) and also after hybridization with t-ssDNA. The dependency of the differences between the cathodic peak currents before and after hybridization on the modifier (quantum dots) percentage is presented in Fig. 4(I). It should be noted that with a 40% of modifier, well-defined peaks were attained neither before nor after hybridization. Based on the results, no peaks appeared in the voltammograms recorded using UCPE, indicating negligible immobilization of (p-ssDNA) on the UCPE surface. In addition, 20% modifier provided the highest cathodic peak current, and this value was chosen to prepare the genosensor. Upon increment in the modifier percentage to 20%, the immobilization units increased and the surface concentration of (p-ssDNA) increased. However, higher percentage caused to decrement in the electrical conductivity of the carbon paste and decrement in the peak current. To optimize the concentration of (p-ssDNA) to immobilize on the MCPE surface, different concentrations of (p-ssDNA) were immobilized on the MCPE surface, and cyclic voltammograms of MB were recorded using (p-ssDNA)-immobilized MCPE, before and after hybridization with t-ssDNA. As it is displayed in Fig. 5(A), 7 μmol L^{-1} (p-ssDNA) solution provided the highest peak current difference. Increment in the concentration of (p-ssDNA) caused to increment in the immobilized concentration of the probe, and a concentration of 7 μmol L^{-1} provided a saturated surface concentration. In order to optimize the hybridization time, the genosensor was prepared and then hybridized with t-ssDNA at different times. The results are shown in Fig. 5(B), and indicate that after 40 min, the (p-ssDNA)–t-ssDNA hybridization process completes, and this time was selected as the best time of hybridization.

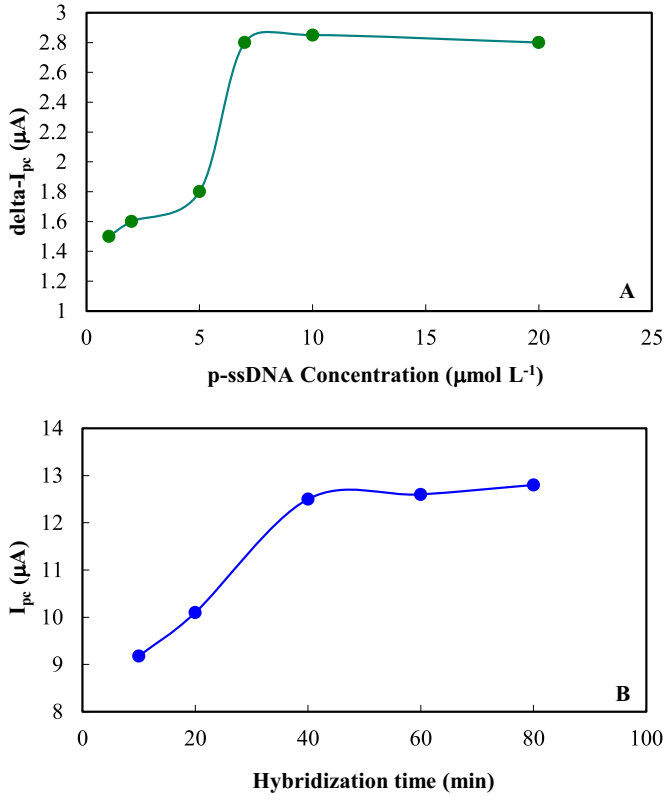

Fig. 5. A)Dependency of the differences between cathodic peak currents of MB in cyclic voltammograms recorded before and after hybridization on the concentration of (p-ssDNA) employed for fabrication of the genosensor. (p-ssDNA)-immobilized electrodes with 10 μL of various concentrations of (p-ssDNA) were fabricated. They were then incubated in a solution containing Tris +20 μmol L^{-1} MB for 5 min at 37 °C, rinsed with Tris to remove the physically absorbed MB, and then cyclic voltammograms were recorded. After that, these electrodes were hybridized with 10 μL of 1.0×10^{-13} μmol L^{-1} t-ssDNA solution dissolved in Tris for 40 min at 37 °C. Afterward, they were incubated in a solution containing Tris +20 μmol L^{-1} MB for 5 min at 37 °C, rinsed with Tris to remove the physically absorbed MB, and then cyclic voltammograms were recorded. B) Dependency of the cathodic peak currents of MB in cyclic voltammograms recorded after hybridization of the genosensor with 10 μL of 1.0×10^{-13} μmol L^{-1} t-ssDNA solution dissolved in Tris for different times at 37 °C. After hybridization of the genosensor with t-ssDNA, the genosensor was incubated in a solution containing Tris +20 μmol L^{-1} MB for 5 min at 37 °C, rinsed with Tris to remove the physically absorbed MB, and then cyclic voltammograms were recorded.

Fig. 6 shows DPVs of MB while interacting with the genosensor before and after hybridization with different concentrations of t-ssDNA recorded in Tris. The curve recorded using MCPE is also shown in Fig. 6. The peak current of MB using MCPE is the lowest, and that for the genosensor is higher. Upon hybridization of the genosensor with t-ssDNA, the peak current increased further. This indicates the interaction of MB with both (p-ssDNA) and the resultant double stranded DNA (dsDNA), with higher affinity to dsDNA. MB binds with both single stranded DNA (ssDNA) and dsDNA through different modes of interactions of hydrophobic and electrostatic [44]. Under the (low) ionic strength of the MB

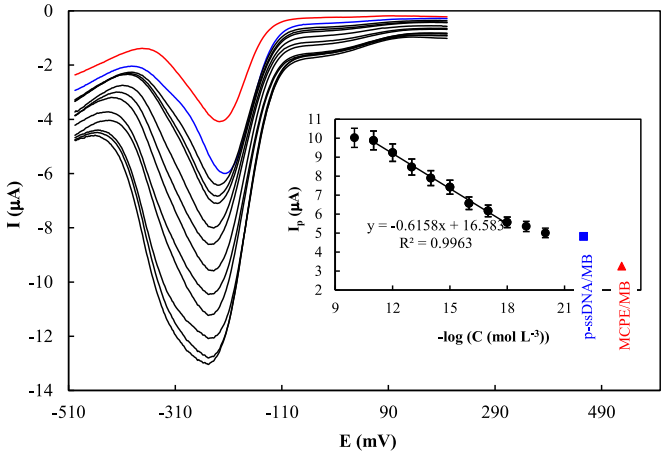

Fig. 6. DPVs of MB interacting with (p-ssDNA) before and after hybridization with different concentrations of t-ssDNA recorded in Tris. Inset: The dependency of the peak current on the t-ssDNA concentration.

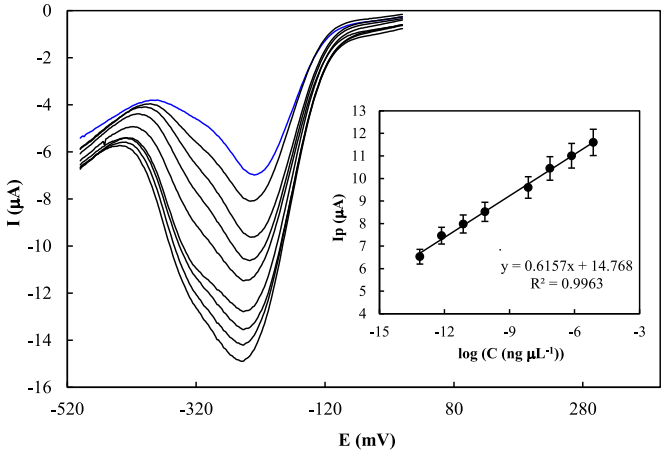

Fig. 7. DPVs of MB while interacting with the genosensor before and after hybridization with different concentrations of genomic target. Inset: The dependency of the peak current on the t-ssDNA concentration.

solution employed here, binding of MB with dsDNA through intercalation is favorable. This behavior was also observed elsewhere [19,44,45]. The dependency of the peak current on the t-ssDNA concentration is shown in Fig. 6, inset. The plot is linear with a regression equation of $y=-(0.6158\pm0.2262)x+(16.583\pm0.0154)$ in the range of 1.0×10^{-11} to 1.0×10^{-18} mol L^{-1} of t-ssDNA with a limit of detection (LOD, as 3 SD/m, SD is the standard deviation of blank signal, and m is the slope of the calibration curve) of 2.0×10^{-19} mol L^{-1} of t-ssDNA.

In order to detect the genomic DNA, DNA genome was extracted from *Leishmania major*, and the DNA concentrations in the extracted samples were determined. Then, solutions of the parasite genome with different concentrations were prepared and placed at 90 °C for 10 min to dehybridize. After that, DPVs of MB while interacting with the genosensor before and after hybridization with different concentrations of genomic target were recorded. The DPVs are shown in Fig. 7, and the corresponding calibration curve is presented in Fig. 7, inset. Based on the obtained results, the genome of *Leishmania major* can be detected in a linear range of 7.31×10^{-14} to 7.31×10^{-6} ng μL^{-1} with a LOD of 1.80×10^{-14} ng μL^{-1}. The LOD value obtained here is lower than some genosensors reported previously [46,47].

To evaluate the selectivity of the genosensor toward other *Leishmania* species, *Leishmania infantum* and *Leishmania tropica* were checked as negative controls. DNA genomes were extracted from these species, and dehybridized. Then, two concentrations of 7.31×10^{-8} and 7.31×10^{-6} ng μL^{-1} from these samples were analyzed with the genosensor. For both these concentrations, the peak currents in DPVs showed slight increment, compared to the peak current for the genosensor (Fig. 8). This indicates that the genosensor can distinguish *Leishmania major* from *Leishmania infantum* and *Leishmania tropica*.

In order to check the applicability of the genosensor for diagnosis of cutaneous leishmaniasis in patients, biopsy specimens of 6 human samples with leishmaniasis were collected and extracted, and PCR and gel electrophoresis were performed. Based on the PCR-gel electrophoresis analyses, the samples included 5 resulting from *Leishmania major* and one resulting from *Leishmania tropica*. The extracted DNA samples (without PCR) were then dehybridized and analyzed using the genosensor. Changes in the peak currents in DPVs were obtained using the genosensor for theses samples. On the other hand, the value of 10 × standard deviation of the peak current for (p-ssDNA) (blank signal, n=3) were obtained and

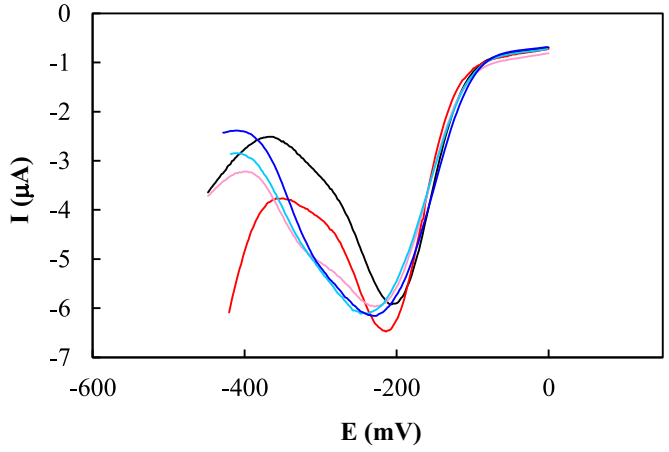

Fig. 8. DPVs of MB while interacting with the genosensor before (black curve) and after hybridization with 7.31×10^{-8} (blue and red curves) and 7.31×10^{-6} ng μL^{-1} (light blue and light red curves) of *Leishmania infantum* (red curves) and *Leishmania tropica* (blue curves). (For interpretation of the references to color in this figure legend, the reader is referred to the web version of this article.)

Table 1
The results obtained for the analysis of extracted DNA samples from patients infected by *Leishmania* species.

Sample No.	Parasite species	SD-$I_{p,\ gen}$ (μA)	10 × SD-$I_{p,\ gen}$ (μA)	$I_{p,\ hyb}$ (μA)
1	*Major*	0.167	1.67	4.88
2	*Major*	0.070	0.70	4.37
3	*Major*	0.180	1.80	4.28
4	*Major*	0.226	2.26	4.44
5	*Major*	0.079	0.79	3.3
6	*Tropica*	0.289	2.89	4.99

SD-$I_{p,\ gen}$: Standard deviation (n=3) of the peak current of MB in DPV recorded in Tris for the genosensor before hybridization with the genomic DNA extracted from patient samples.
$I_{p,\ hyb}$: The peak current of MB in DPV recorded in Tris for the genosensor after hybridization with the genomic DNA extracted from patient samples.

presented in Table 1. It was found that the increments in the peak currents for the samples containing *Leishmania major* were significant (higher than the limit of quantitation of the genosensor), and that for *Leishmania tropica* it was non-significant. The results indicated that this label-free, PCR-free, signal-on genosensor is capable to detect *Leishmania major* in the samples from patients without amplification.

4. Conclusion

1. A simple precipitation procedure was developed for the synthesis of cobalt substituted zinc ferrite quantum dots.
2. The quantum dots were evaluated for the immobilization of a *Leishmania*-specific probe without any functionalization (such as thiolation, biotinylation); the results indicated that ssDNA had a high affinity to the surface of the quantum dots.
3. The quantum dots had an electrocatalytic activity toward the electroreduction of MB, resulting in the enhancement in the genosensor signals and sensitivity. The quantum dots had a great potential to fabricate DNA biosensors.
4. The fabricated label-free, PCR-free and signal-on genosensor showed a high sensitivity to detect cutaneous leishmaniasis.

Acknowledgments

The paper has been extracted from the F. Reisi M. Sc. thesis supported by the Research Council of Shiraz University of Medical Sciences (7375). We would also like to thank the Iran National Science Foundation (INSF) for supporting this research, and Prof. A. Khamesipour for his valuable assistances.

References

[1] P.A. Kitchin, Z. Szotyori, C. Fromholc, N. Almond, Avoidance of PCR false positives, Nature 344 (1990) 201.
[2] S. Kwok, R. Higuichi, Avoiding false positives with PCR, Nature 339 (1989) 237–238.
[3] A.M. Prince, L. Andrus, PCR: how to kill unwanted DNA, Biotechniques 12 (1992) 358–359.
[4] B. Duan, J.J. Zhou, Z. Fang, C.X. Wang, X.J. Wang, H.F. Hemond, M.B. Chan-Park, H.W. Duan, Surface enhanced Raman scattering by graphene-nanosheet-gapped plasmonic nanoparticle arrays for multiplexed DNA detection, Nanoscale 7 (2015) 12606–12613.
[5] A. Bandyopadhyay, K. Sarkar, Localized surface plasmon resonance-based DNA detection in solution using gold-decorated superparamagnetic Fe_3O_4 nanocomposite, Anal. Biochem. 465 (2014) 156–163.
[6] J.J. Ahn, S.Y. Lee, J.Y. Hong, Y. Kim, G.W. Kim, S.Y. Hwang, Application of fluorescence melting curve analysis for dual DNA detection using single peptide nucleic acid probe, Biotechnol. Prog. 31 (2015) 730–735.

[7] N. Sattarahmady, G.H. Tondro, M. Golchin, H. Heli, Gold nanoparticles biosensor of Brucella spp. genomic DNA:Visual and spectrophotometric detections, Biochem. Eng. J. 97 (2015) 1–7.
[8] A. Rahi, N. Sattarahmady, H. Heli, Zepto-molar electrochemical detection of Brucella genome based on gold nanoribbons covered by gold nanoblooms, Sci. Rep. (5) , Article number 18060.
[9] L. Wu, E. Xiong, X. Zhang, X. Zhang, J. Chen, Nanomaterials as signal amplification elements in DNA-based electrochemical sensing, Nano Today 9 (2014) 197–211.
[10] J.P. Tosar, G. Branas, J. Laiz, Electrochemical DNA hybridization sensors applied to real and complex biological samples, Biosens. Bioelectron. 26 (2010) 1205–1217.
[11] J. Wang, X. Cai, G. Rivas, H. Shiraishi, P.A.M. Farias, N. Dontha, DNA electrochemical biosensor for the detection of short DNA sequences related to the human immunodeficiency virus, Anal. Chem. 68 (1996) 2629–2634.
[12] A. Rahi, K. Karimian, H. Heli, Nanostructured materials in electroanalysis of pharmaceuticals, Anal. Biochem. 497 (2016) 39–47.
[13] H. Heli, N. Sattarahmady, A. Jabbari, A.A. Moosavi-Movahedi, G.H. Hakimelahi, F.Y. Tsai, Adsorption of human serum albumin onto glassy carbon surface-Applied to albumin-modified electrode: mode of protein-ligand interactions, J. Electroanal. Chem. 610 (2007) 67–74.
[14] H. Heli, A.A. Moosavi-Movahedi, A. Jabbari, F. Ahmad, An electrochemical study of safranin O binding to DNA at the surface, J. Solid State Electrochem. 11 (2007) 593–599.
[15] D. Bas, I.H. Boyaci, Photoelectrochemical competitive DNA hybridization assay using semiconductor quantum dot conjugated oligonucleotides, Anal. Bioanal. Chem. 400 (2011) 703–707.
[16] A.G. Pershina, A.E. Sazonov, L.M. Ogorodova, Investigation of the interaction between DNA and cobalt ferrite nanoparticles by FTIR spectroscopy, Russ. J. Bioorgan. Chem. 35 (2009) 607–613.
[17] M.H. Alshehri, B.J. Cox, J.M. Hill, DNA adsorption on graphene, Eur. Phys. J. 67D (2013) 226–234.
[18] J.H. Kim, J.H. Jin, J.Y. Lee, E.J. Park, N.K. Min, Covalent attachment of biomacromolecules to plasma-patterned and functionalized carbon nanotube-based devices for electrochemical biosensing, Bioconjug. Chem. 23 (2012) 2078–2086.
[19] M. Liu, C. Luo, H. Peng, Electrochemical DNA sensor based on methylene blue functionalized polythiophene as a hybridization indicator, Talanta 88 (2012) 216–221.
[20] X.N. Zhang, H.M. Hu, DNA molecules site-specific immobilization and their applications, Cent. Eur. J. Chem. 12 (2014) 977–993 (and references therein).
[21] R. Meyer, S. Giselbrecht, B.E. Rapp, M. Hirtz, C.M. Niemeyer, Advances in DNA-directed immobilization, Curr. Opin. Chem. Biol. 18 (2014) 8–15 (and references therein).
[22] P. He, Y. Xu, Y. Fang, Applications of carbon nanotubes in electrochemical DNA biosensors, Microchim. Acta 152 (2006) 175–186.
[23] A. Erdem, Nanomaterial-based electrochemical DNA sensing strategies, Talanta 74 (2007) 318–325.
[24] H.S. Nalwa, Encyclopedia of Nanoscience and Nanotechnology, American Scientific Publishers, 2001.
[25] H. Heli, O. Amirizadeh, Non-enzymatic glucose biosensor based on hyperbranched pine-like gold nanostructure, Mater. Sci. Eng. C 63 (2016) 150–154.
[26] N. Sattarahmady, H. Heli, R. Dehdari Vais, A flower-like nickel oxide nanostructure: Synthesis and application for choline sensing, Talanta 119 (2014) 207–213.
[28] R. Dehdari Vais, N. Sattarahmady, K. Karimian, H. Heli, Green electrodeposition of gold hierarchical dendrites of pyramidal nanoparticles and determination of azathioprine, Sens. Actuators B 215 (2015) 113–118.
[29] T.A.P. Rocha-Santos, Sensors and biosensors based on magnetic nanoparticles, Trends Anal. Chem. 62 (2014) 28–36.
[30] I. Giouroudi, F. Keplinger, Microfluidic biosensing systems using magnetic nanoparticles, Int. J. Mol. Sci. 14 (2013) 18535–18556.
[31] P. Desjeux, Leishmaniasis: current situation and new perspectives, Comp. Imunnol. Microbiol. Infect. Dis. 27 (2004) 305–318.
[32] P. Desjeux, Leishmaniasis, Nat. Rev. Microbiol. 2 (2004) 692.
[33] T. Kobets, I. Grekov, M. Lipoldova, Leishmaniasis: prevention, parasite detection and treatment, Curr. Med. Chem. 19 (2012) 1443–1474.
[34] M. Paiva-Cavalcanti, C.G. Regis-da-Silva, Y.M. Gomes, Comparison of real-time PCR and conventional PCR for detection of Leishmania (Leishmania) infantum infection: a mini-review, J. Venom. Anim. Toxins. Incl. Trop. Dis. 16 (2010) 537–542.
[35] L. Solano-Gallego, A. Rodriguez, L. Iniesta, M. Arboix, M. Portus, J. Alberola, Detection of *anti*-Leishmania immunoglobulin G antibodies in urine specimens of dogs with leishmaniasis, Clin. Diagn. Lab. Immun. 10 (2003) 849–855.
[36] R. Houghton, Emergency Characterization of Unknown Materials, CRC Press 2007, p. 215.
[37] B. Byrne, E. Stack, N. Gilmartin, R. O'Kennedy, Antibody-based sensors: principles, problems and potential for detection of pathogens and associated toxins, Sensors 9 (2009) 4407–4445.
[38] S. Khademvatan, N. Neisi, S. Maraghi, J. Saki, Diagnosis and identification of *Leishmania* spp. From Giemsa-stained slides, by real-time PCR and melting curve analysis in south-west of Iran, Ann. Trop. Med. Parasitol. 105 (2011) 559–565.
[39] M. Zuker, Mfold web server for nucleic acid folding and hybridization prediction, Nucleic Acids Res. 33 (2003) 3406–3415.
[40] A.J. Bard, L.R. Faulkner, Electrochemical Methods, 2nd ed., John Wiley And Sons, NewYork, 2001.
[41] A.G. Pershina, A.E. Sazonov, L.M. Ogorodova, Evaluation of the resistance of DNA immobilized on ferrimagnetic particles of cobalt ferrite nanopowder against nuclease cleavage, Bull. Exp. Biol. Med. 149 (2010) 67–69.
[42] J. Prodelalova, B. Rittich, A. Spanova, K. Petrova, M.J. Benes, 1056, 2004, pp. 43–48.
[43] J.H. Nam, Y.H. Joo, J.H. Lee, J.H. Chang, J.H. Cho, M.P. Chun, B.I. Kim, Preparation of NiZn-ferrite nanofibers by electrospinning for DNA sep, J. Magn. Magn. Mater. 321 (2009) 1389–1392.
[44] E. Farjami, L. Clima, K.V. Gothelf, E.E. Ferapontova, DNA interactions with a Methylene Blue redox indicator depend on the DNA length and are sequence specific, Analyst 135 (2010) 1443–1448.
[45] S. Radhakrishnan, C. Sumathi, V. Dharuman, J. Wilson, Polypyrrole nanotubes-polyaniline composite for DNA detection using methylene blue as intercalator, Anal. Methods 5 (2013) 1010–1015.
[46] M. Andreadou, E. Liandris, M. Gazouli, S. Taka, M. Antoniou, G. Theodoropoulos, I. Tachtsidis, N. Goutas, D. Vlachodimitropoulos, I. Kasampalidis, J. Ikonomopoulos, A novel non-amplification assay for the detection of Leishmania spp. in clinical samples using gold nanoparticles, J. Microbiol. Methods 96 (2014) 56–61.
[47] S. Mohan, P. Srivastava, S.N. Maheshwari, S. Sundar, R. Prakash, Nano structured nickel oxide based DNA biosensor for detection of visceral leishmaniasis (Kala-azar), Analyst 136 (2011) 2845–2851.